Int. J. Solids Structures, 1974, Vol. 10, pp. 945–956. Pergamon Press. Printed in Gt. Britain.

ELASTIC–PLASTIC ANALYSIS OF A WHEEL ROLLING ON A RIGID TRACK†

VIJAY K. GARG‡

Electromotive Division General Motors Corporation, Lagrange, Illinois 60559, U.S.A.

SUBHASH C. ANAND§

Clemson University, Clemson, South Carolina 29631, U.S.A.

and

PHILIP G. HODGE, JR.‖

University of Minnesota, Minneapolis, Minnesota 55455, U.S.A.

(*Received* 26 *October* 1973; *revised* 15 *January* 1974)

Abstract—A consistent finite element model for a circular wheel is developed based on triangular and quasi-triangular domains and a piecewise linear displacement field. The minimum stress-rate principle of plasticity is used to obtain the solution of this two-dimensional continuum problem with internal unloading. A piecewise approximation of the Tresca yield condition is used. Elastic–plastic solutions of a wheel rolling on a rigid track under its own weight and a hub load are obtained for the first few revolutions until a steady state condition is reached. Shake-down conditions for the wheel are demonstrated.

1. INTRODUCTION

When a wheel which is either heavy with its own weight or which carries a heavy hub load rolls on a straight track, both the wheel and the track will deform and there will generally be a highly stressed region in both of them near the area of contact. As a first step in the analysis of this problem we assume that the track is substantially stronger than the wheel and we focus our attention on the latter.

As the wheel rolls, the highly stressed region of the wheel will change and the original highly stressed region will unload. However, after a rotation of 360° the load system will be the same as it was initially. If the entire process has been elastic, the solution at 360° will be identical with the initial solution, so that the wheel will immediately achieve a steady state.

† This investigation was supported by the Office of Naval Research and by the National Science Foundation while all three authors were associated with Illinois Institute of Technology.

‡ Senior Project Engineer.

§ Associate Professor of Civil Engineering.

‖ Professor of Mechanics.

However, let us consider the case where the loads are sufficiently great to cause plastic behavior during the first revolution, but not so great that plastic collapse occurs. Then, as the wheel rolls, the initially highly stressed plastic region will unload elastically. Since plastic unloading follows a different law than plastic loading, there will be a non-zero residual stress state after a complete revolution and the stress distributions at 360° and 0° will not be identical. A similar remark will apply to each subsequent revolution, but we would intuitively expect that the wheel would soon approach a steady state in which conditions at a total rotation angle of $(\theta + 360\ n)^\circ$ were independent of n for n sufficiently large.

If this steady state exists, it may involve purely elastic behavior even though the initial state was partially plastic or it may involve plastic behavior with each revolution. In the latter case, the capacity of the wheel to absorb plastic work will soon be exhausted and the material of the wheel may be expected to fail. Obviously, this state of affairs is to be avoided in any practical design. However, if the steady state solution is purely elastic, it is probable that no serious damage was done to the wheel by the first few plastic revolutions.

Our concern, then is to investigate the elastic–plastic behavior of the wheel during the first few revolutions until a steady state is reached. An exact solution of this problem would be exceedingly difficult to obtain and we shall begin by constructing a greatly simplified model of the problem which will retain its most important factors. The model will be described in detail in Section 2, but its essential features are easily stated.

The track will be taken as rigid and the wheel assumed to be in a state of plane stress. The material of the wheel will be assumed to be elastic-perfectly plastic with a piecewise linear yield condition. A finite element model will be used for the wheel and the loads will be approximated by ones which are piecewise linear in time when viewed from a reference system which moves with the wheel.

In Section 3 we will formulate the stress rate problem and describe a method for its solution and for its integration in time to obtain the stresses. Section 4 will present some specific results and the paper will close by discussing some conclusions to be drawn from the investigation.

2. MATHEMATICAL MODEL

In the two-dimensional continuum model the wheel is represented by a circle. The finite element model is obtained by first assigning a node at the center and connecting it to n_p equispaced nodes along the circumference, thus dividing the circle into n_p sectors. Each sector is then further divided into m_s, 3-sided domains A^k, the pattern being the same in each sector and symmetric with respect to the center line of the sector. Each A^k is determined by 3 nodes and nodes may be on the circumference of the circle or in its interior. A side of A^k between two circumferential nodes is the portion of the circle between those nodes; all other sides are straight. Obviously, the total number of domains is $M = n_p m_s$. We shall denote by N and S the total number of nodes and edges, respectively.

Figure 1 shows the case $n_p = 3$, $m_s = 4$. Thus, $M = 12$ and evidently $N = 10$ and $S = 21$. Domains A^7–A^{12} have one circular and two straight sides; the other domains are triangular.

Following Hodge[1], we use the principle of virtual work to establish the generalized variables and defining equations. The displacement vector at node λ is denoted by† ψ_α^λ and the complete set of ψ_α^λ uniquely determines a continuous, piecewise linear displacement field

† Greek subscripts have the range 1, 2 and follow the summation convention.

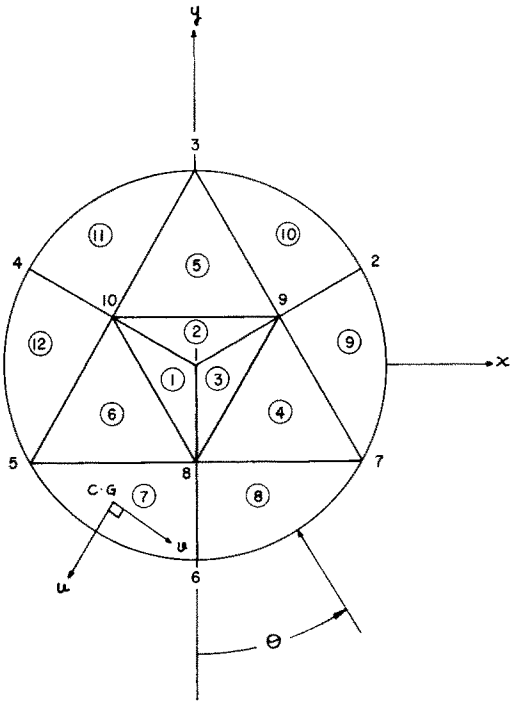

Fig. 1. Finite element model of wheel.

over the wheel. Let $u_\alpha^k(x_1, x_2)$ denote this field in A^k. Then the generalized strains for the wheel are the set of $3M$ constants defined in A^k by

$$\varepsilon_{\alpha\beta}^k = \frac{1}{2}\frac{A^k}{A_0}(u_{\alpha,\beta}^k + u_{\beta,\alpha}^k). \tag{2.1}$$

Here A_0 is the area of wheel and A^k denotes its own area.

Next we define a dimensionless generalized stress set of $3M$ constants by

$$\sigma_{\alpha\beta}^k = \frac{1}{A^k\sigma_0}\int_{A^k} \sigma_{\alpha\beta}\,\mathrm{d}A. \tag{2.2}$$

Where σ_0 is the yield stress of the material. The set of constants (2.1) and (2.2) obviously satisfy Prager's criterion[2] for generalized variables.

The wheel may be loaded by its own weight, by a concentrated load at the hub, and by the reaction due to track. As shown in [1] the finite element model replaces the continuum load distribution by a set of concentrated loads at the nodes given by

$$G_\alpha^\lambda = C_\alpha^\lambda + \sum_r^\lambda \int [f_\alpha(x, y)L^r(x, y)/L^r(x^\lambda, y^\lambda)]\,\mathrm{d}A. \tag{2.3}$$

Here C_α^λ is the concentrated load applied to the node, $\sum_r^\lambda$ denotes the sum over all domains A^r which have λ as one of their nodes, f_α is the external load vector, and $L^r(x, y)$ is the linear factor

$$L^r = \frac{1}{2}\begin{vmatrix} x & y & 1 \\ x' & y' & 1 \\ x'' & y'' & 1 \end{vmatrix}$$

where (x', y') and (x'', y'') are the coordinates of the other two vertices of domain A^r. For a triangle, $L^r(x^\lambda, y^\lambda) = A^r$, but this is not true if any of the sides are curved. Equation (2.3) was derived in[1] only for triangular domains, but it is equally valid for the curvilinear triangles which include the boundary. The integration is to be performed for all external loads including the weight of the wheel and the reaction of the track.

For the real physical wheel, the effect of the load will be to induce a deformation of the wheel so that a finite length of it will be in contact with the rail. The reaction load will be distributed over this small length in an unknown fashion to be determined by the boundary conditions on displacements. However, since the reaction load enters the finite element computations only through the integration in equation (2.3), it is evident that the details of load distribution there will be relatively unimportant. Therefore, we consider the reaction force to act as a concentrated load at the single point of contact of the undeformed wheel with the track.

We find it convenient to keep coordinates fixed in the wheel. If θ represents the total angle through which the wheel has rolled from an initial position with the y-axis vertically upward, the components of the body force per unit area, concentrated hub load, and reaction force will be, respectively,

$$f_\alpha = w_d(\sin\theta, -\cos\theta) \tag{2.4a}$$

$$H_\alpha = F(\sin\theta, -\cos\theta) \tag{2.4b}$$

$$T_\alpha = (\pi R^2 w_d + F)(-\sin\theta, \cos\theta). \tag{2.4c}$$

Here w_d is the surface density, F is the magnitude of the hub load and R is the radius of the wheel.

When equations (2.4) are substituted in equation (2.3), it is obvious that the resulting nodal load components will be trignometric functions of θ:

$$G_\alpha^\lambda = \phi^\lambda(\sin\theta, -\cos\theta). \tag{2.5}$$

As will be seen later, the complete solution to the problem will involve integration of numerically determined results with respect to θ. Although this is not difficult to do to any desired degree of approximation based on (2.5), it is conceptually simpler and has certain advantages in comparing and interpreting results, if we first replace (2.5) by a load history which is piecewise linear in time. Therefore, we fix an interval $\Delta\theta$ and define a discrete set of values $\theta_n = n\,\Delta\theta$. Then in each interval $\theta_n < \theta < \theta_{n+1}$ the load rate is taken to be the constant

$$\dot{G}_\alpha^\lambda = [G_\alpha^\lambda(\theta_{n+1}) - G_\alpha^\lambda(\theta_n)]/\Delta\theta. \tag{2.6}$$

Finally, the load system (2.5) is replaced by the piecewise linear load system

$$F_\alpha^\lambda = G_\alpha^\lambda(\theta_n) + (\theta - \theta_n)\dot{G}_\alpha^\lambda \qquad \theta_n < \theta < \theta_{n+1}. \tag{2.7}$$

As shown in[1], substitution of (2.1), (2.2) and (2.7) into the Principle of Virtual Work leads to the $2N$ equilibrium equations.

$$\sum_{r}^{\lambda} \frac{1}{2} \frac{A^r}{L^r(x^\lambda, y^\lambda)} [\sigma^r_{\alpha 1}(y' - y'') + \sigma^r_{\alpha 2}(x'' - x')] = F^\lambda_\alpha/\sigma_0 . \tag{2.8}$$

Any set of $3M$ constants $\sigma^k_{\alpha\beta}$ and $2N$ constants F^λ_α which satisfy the $2N$ equations (2.8) will be called a statically consistent set.

As shown in[3], the elastic–plastic constitutive equations for the finite element model have the same form as for the continuum. Thus, if the wheel material has a yield condition $f(\sigma_{\alpha\beta}) \leq 0$ and satisfies Drucker's postulates[4], the model variables must satisfy

$$\dot{\varepsilon}^k_{\alpha\beta} = \dot{e}^k_{\alpha\beta} + \dot{p}^k_{\alpha\beta} \tag{2.9a}$$

$$\dot{e}^k_{\alpha\beta} = C^k_{\alpha\beta\lambda\mu} \dot{\sigma}^k_{\lambda\mu} \tag{2.9b}$$

$$f(\sigma^k_{\alpha\beta}) \leq 0 \tag{2.9c}$$

$$(\sigma^k_{\alpha\beta} - \sigma^{k*}_{\alpha\beta})\dot{p}^k_{\alpha\beta} \geq 0 \tag{2.9d}$$

$$\dot{\sigma}^k_{\alpha\beta}\, \dot{p}^k_{\alpha\beta} = 0. \tag{2.9e}$$

Here $\dot{e}^k_{\alpha\beta}$ and $\dot{p}^k_{\alpha\beta}$ denote the elastic and plastic strain rates, $\sigma^{k*}_{\alpha\beta}$ is any other stress state which satisfies (2.9c), $C^k_{\alpha\beta\lambda\mu}$ is defined as

$$C^k_{\alpha\beta\lambda\mu} = \sigma_0 \frac{A^k}{A_0} C_{\alpha\beta\lambda\mu} \tag{2.10}$$

where $C_{\alpha\beta\lambda\mu}$ is the symmetric tensor of elastic constants of the material.

The Tresca yield condition is represented geometrically by a circular cylinder with conical caps. The axis of the figure is $\sigma^k_{11} = \sigma^k_{22}$, $\sigma^k_{12} = 0$; the cylinder has a radius of 1/2 and lies between the planes $\sigma^k_{11} + \sigma^k_{22} = \pm 1$; the caps have vertices at $\sigma^k_{11} = \sigma^k_{22} = \pm 1$, $\sigma^k_{12} = 0$ and intersect the cylinder at its bounding planes. For our model we replace the circular cylinder and cones by a hexagonal prism and pyramids, thus leading to an 18-sided polygon

$$b^i_{\alpha\beta}\, \sigma^k_{\alpha\beta} - 1 = 0 \qquad i = 1, 2, \ldots, 18 \tag{2.11}$$

where $b^i_{\alpha\beta}$ are listed in Table 1.

Although the Tresca yield condition is isotropic, the approximation (2.11) is not. In order to minimize the effect of this induced anisotropy in the model, the "yield axes" in each finite element are chosen to be radial and circumferential through the center of gravity of the element (Fig. 1).

3. SOLUTION

The stress solution is found as a function of time by determining the stress rates at a certain instant, integrating to find the stresses at a later instant, and continuing this process To determine the stress rates, we consider the class of all "statically admissible" rate states which satisfy the rate form of (2.8) and the constraints

$$IF\ b^i_{\alpha\beta}\, \sigma^k_{\alpha\beta} = 1 \quad \text{THEN} \quad b^i_{\alpha\beta}\, \dot{\sigma}^k_{\alpha\beta} \leq 0 \tag{3.1}$$

Table 1. Values of $b^i_{\alpha\beta}$, equation (2.11)

Plane	$2\sqrt{3}\,b^i_{11}$	$2\sqrt{3}\,b^i_{22}$	$2b^i_{12}$
a	2	2	2
b	4	−4	0
c	2	−2	−2
d	−2	2	−2
e	−4	4	0
f	−2	2	2
g	$\sqrt{3}+1$	$\sqrt{3}-1$	1
h	$\sqrt{3}+2$	$\sqrt{3}-2$	0
j	$\sqrt{3}+1$	$\sqrt{3}-1$	−1
k	$\sqrt{3}-1$	$\sqrt{3}+1$	−1
l	$\sqrt{3}-2$	$\sqrt{3}+2$	0
m	$\sqrt{3}-1$	$\sqrt{3}+1$	1
n	$-\sqrt{3}+1$	$-\sqrt{3}-1$	1
p	$-\sqrt{3}+2$	$-\sqrt{3}-2$	0
q	$-\sqrt{3}+1$	$-\sqrt{3}-1$	−1
r	$-\sqrt{3}-1$	$-\sqrt{3}+1$	−1
s	$-\sqrt{3}-2$	$-\sqrt{3}+2$	0
t	$-\sqrt{3}-1$	$-\sqrt{3}+1$	1

which are implied by (2.9c). Then, as shown in[5], the actual rate solution minimizes

$$\pi_c = \frac{1}{2}\sum_{k=1}^{M} C^k_{\alpha\beta\lambda\mu}\,\dot\sigma^k_{\alpha\beta}\,\dot\sigma^k_{\lambda\mu} \tag{3.2}$$

among all statically admissible rate states.

This problem is known as "quadratic programming" and known mathematical procedures are available for its solution. Once the rates are known for some generic time† $\bar\theta$, the stresses at a later time $\bar\theta + \delta\theta$ can be computed from

$$\sigma^k_{\alpha\beta}(\bar\theta + \delta\theta) = \sigma^k_{\alpha\beta}(\bar\theta) + \delta\theta\dot\sigma^k_{\alpha\beta}\,. \tag{3.3}$$

Equation (3.3) is generally just an approximation. However, due to the piecewise linear nature of the model problem, it is exact provided that the load rate (2.6) is constant and no element enters a new plastic regime. Thus, if $\theta_n \le \bar\theta < \theta_{n+1}$ we require first that $\delta\theta$ satisfy

$$\bar\theta + \delta\theta \le \theta_{n+1}\,. \tag{3.4a}$$

Further, for each element and yield face for which $b^i_{\alpha\beta}\,\sigma^k_{\alpha\beta}(\bar\theta) < 1$, we require that $\delta\theta$ satisfy

$$b^i_{\alpha\beta}[\sigma^k_{\alpha\beta}(\bar\theta) + \delta\theta\dot\sigma^k_{\alpha\beta}] \le 1. \tag{3.4b}$$

Therefore, we choose $\delta\theta$ to be the largest number satisfying all of (3.4) whence (3.3) determines the stresses exactly at time $\bar\theta + \delta\theta$.

To start the solution, the wheel is regarded as not rolling ($\theta = 0$) while the load magnitude $\phi(t)$ is slowly increased at a constant rate to its final value. For this stage ϕ replaces θ as the time variable. Initially all stresses and loads are zero. The quadratic programming problem

† Since perfectly plastic flow is quasi-static we can choose the rotation θ as our time variable.

is solved for the stress rates, and $\delta\phi$ is determined from formulas analogous to (3.4). Then, with $\bar{\phi} = \delta\phi$ the process is repeated and continued until the load reaches its full value with a stress distribution denoted by $\sigma^k_{\alpha\beta}(0)$. Rates with respect to θ are computed, $\delta\theta$ is found from (3.4) and stresses are found at $\bar{\theta} = \delta\theta$. Continuing this process, we can find the stress distribution at any finite time in a finite number of steps.

4. RESULTS

A computer program was written to study the elastic–plastic behavior of the wheel. A quadratic programming routine[6] based on the simplex method was used to compute the elastic solution and collapse loads for the wheel, and to solve the stress-rate problem. The program was first tested with a three-element model of the wheel, but all the results reported in this section are for the 12-element model† shown in Fig. 1. Loading conditions. were gravity load only and hub load only.

Although the real wheel is fully symmetric with regard to position, the model exhibits only 60° symmetry. Therefore on initial loading the maximum elastic load factor and the collapse load factor will vary with the initial orientation of the wheel, Fig. 2. The extent of these variations is one measure of the error introduced by the model.

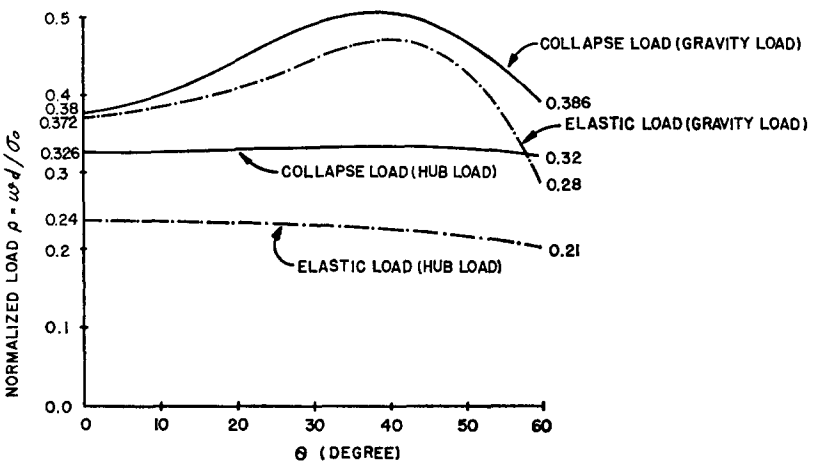

Fig. 2. Elastic and collapse loads for model.

Since the wheel will rotate under constant load magnitude after initial loading and since superposition holds for fully elastic behavior, the maximum elastic load factor ρ^e (ρ is defined as w_d/ρ_0) is the minimum value over all orientations. Similarly, since plastic collapse is independent of history, ρ^c is the minimum plastic collapse factor over all orientations.

Once ρ^e and ρ^c were computed, the initial position was arbitrarily taken at $\theta = 0$, a load ρ between ρ^e and ρ^c was applied and a history of the wheel rolling under load ρ was computed. For various values of ρ it was found that after only a few revolutions the wheel

† Computer limitations prohibited consideration at a more realistic model. This aspect is discussed further in Section 5.

reached a steady state in which stress history was repeated in each revolution. For loads near ρ^e this steady state was purely elastic even though plastic flow occurred prior to steady state, whereas for loads near ρ^c there was plastic flow in each revolution in the steady state. We consider in some detail the case of gravity loading under the loads $\rho = 0{\cdot}34$ or $\rho = 0{\cdot}35$. We note from Fig. 2, that for either magnitude the initial load application is fully elastic, and that the loads are both between the elastic load $\rho^e = 0{\cdot}28$ and the collapse load $\rho^c = 0{\cdot}38$.

The stress histories are illustrated in Fig. 3 for the first four revolutions, the fourth being steady state in each case. Each line of the figure denotes one revolution according to the scale at the bottom and the upper and lower halves refer to the loads 0·34 and 0·35 respectively. Clear regions indicate that the wheel is fully elastic and the shaded portions indicate periods of partial plasticity. The numbers show which of the elements defined in Fig. 1 are plastic and the lower-case letters denote the plastic regions defined in Table 1.

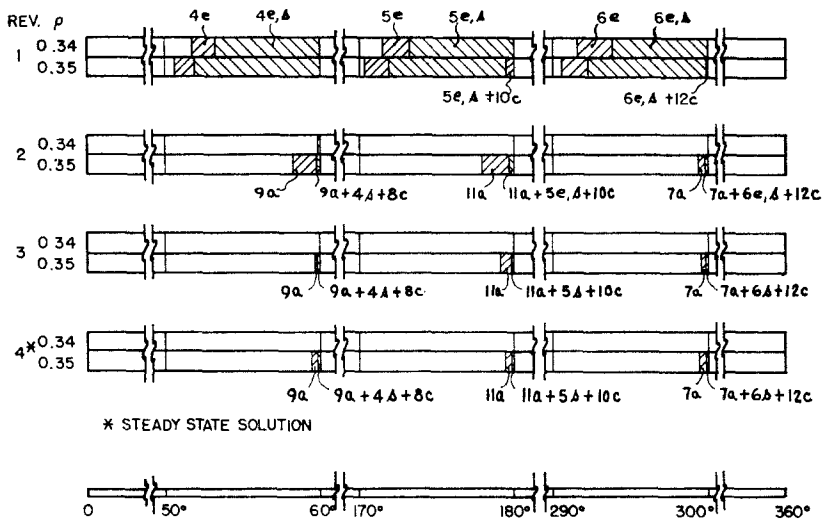

Fig. 3. Stress history under gravity load.

For $\rho = 0{\cdot}34$, the wheel was partly plastic for 25° of the first revolution, for less than 1° during the second revolution and reached a purely elastic steady state by the third revolution. For $\rho = 0{\cdot}35$, the plastic duration is increased about 10 per cent over the duration for 0·34 during the first revolution, steady state is not reached until the fourth revolution and from then on the wheel is partly plastic during about 2° of each revolution. It is interesting to note that during the initial revolution the plastic deformation is confined to the elements 4, 5, 6 which are essentially interior elements. On the other hand, in subsequent revolutions when $\rho = 0{\cdot}35$, most of the plastic deformation is in elements 7, 9, 11 which are on the boundary. Also, although the geometry is symmetric every 60°, there is a definite influence of the direction of rolling in that elements 8, 10, 12 on the boundary are plastic during less of the revolution than are 7, 9, 11.

The initial revolution and the steady state both show the expected 120° symmetry, but this is not true of the intermediate stages. This would indicate that the cross influence of plastic behavior in part of the wheel on later plastic flow in another is slight, but that it is noticeable in the period just prior to steady state.

5. CONCLUSIONS

When a loaded wheel rolls on a straight track, an unknown pressure distribution takes place along an unknown contact region and both the wheel and track are deformed accordingly. This is a mixed boundary value problem with the following boundary conditions. On some undetermined portion of the boundary of the two bodies the displacements are compatible and the contact stresses are in equilibrium. On the other portions of the boundary the forces are prescribed to be zero.

The above defined boundary value problem is obviously a complex one, particularly if the contact force is sufficiently great to cause some plastic behavior in the wheel or track. In an effort to gain some insight into this problem, we have focused our attention on the wheel and have adopted a greatly simplified two-dimensional model in which the track is rigid, the wheel is composed of a finite number of constant strain triangular elements, and all loads (including the contact force) are independent of the deformations and are piecewise linear in time.

In assessing the value of the model, we attempt to analyze how well it predicts important features of behavior of the real wheel. If the real load is less than some critical value $\bar{\rho}^e$, the wheel will always remain elastic; if the load exceeds some value $\bar{\rho}^c$, the wheel will undergo excessive deformations on initial loading and will collapse. For loads between these two values, plastic strains will occur near the contact area on the initial loading and during the initial revolution. As the wheel turns, the earlier contact area will unload but will contain residual stresses. During a second revolution, these residual stresses will affect the stresses during the second contact period which may be either plastic or elastic. Experience suggests that after some finite number of revolutions, a steady state will be reached. Further, for loads only slightly above $\bar{\rho}^e$ we would expect this steady state to be elastic, whereas for loads close to $\bar{\rho}^c$ it would probably involve some plastic flow in each revolution. The load $\bar{\rho}^s$ which separates these two types of behavior represents a significant description of the true strength of the wheel since continued plastic straining will soon cause failure due to plastic fatigue or unbounded plastic deformation, whereas a finite amount of plastic behavior prior to an elastic state will probably not impair its usefulness.

The model does predict loads ρ^e and ρ^c. For a variety of loads between ρ^e and ρ^c a complete analysis was carried out and in every case steady state was achieved in less than five revolutions. The shakedown load ρ^s was approximated by trial and error. Two different loadings were considered (gravity only and hub only) and results were obtained for the 12-element model (Fig. 1) and for an even more crude model of three 120° sectors. Table 2 shows the results for the three critical loads.

The wide variation of numbers in Table 2 indicates that there is little basis for making quantitative predictions of critical loads for the real wheel. Considering what a poor approx-

Table 2. Comparison between 12-element and 3-element models

Load	Gravity		Hub	
Elements	12	3	12	3
ρ^e	0·28	0·57	0·21	0·38
ρ^s	0·34	0·64	0·24	0·45
ρ^c	0·38	0·69	0·32	0·48

mation 12 triangular elements are to a circle, this result is hardly surprising. Based on the results obtained to date, we can only tentatively say that the shakedown load is probably somewhere in the middle third of the range between the elastic and collapse loads.

Another basis for assessing the value of the model is the predicted symmetry of the results. The real wheel is completely rotationally symmetric except that the initial loading takes place in a specific orientation. The 12-element model exhibits only 60° symmetry and the 3-element model is symmetric for 120°. In both models the elastic load ρ^e and the collapse load ρ^c vary with the initial orientation. However, the model does show a complete 120° symmetry for the stresses.

Table 3. Comparison between model and the real wheel

Feature	Model	Reality
1. Strains and stresses	Piecewise constant	Continuously varying
2. Contact force	Concentrated	Distributed
3. Force–time behavior	Piecewise	Sinusoidal
4. Yield condition	Piecewise linear anisotropic	Non-linear isotropic
5. Track	Rigid	Deformable

The model differs from reality in several features, as indicated in Table 3. Of these features the first appears to be by far the most important. Contact stresses and strains are generally very highly localized, so that any piecewiseconstant approximation will introduce a relatively large error. Obviously it would be desirable to analyze a wheel with more elements since this would presumably lead to a closer approximation to the true distribution.

In any finite element scheme, all loads are effectively replaced by equivalent nodal forces so that features 2 and 3 regarding the loads will introduce little additional error. Since the 15° approximation still provides 4 time-steps per element, it is certainly reasonable for the 12-element model.

The piecewise linear yield condition can be made as close to the real one as desired. The maximum effect of this approximation on ρ^e and ρ^c can be accurately estimated, and it is not significant. The anisotropic feature is closely related to the number of elements. The favored direction is precisely radial at each element's center, hence this error will also decrease with more elements.

Finally, from the viewpoint of wheel analysis, the assumption on the track really only affects feature 2 which has already been shown to be insignificant.

Two features of the model itself are worth commenting on. Many schemes for solving finite element problems are based on direct solution of the defining equations (2.8) and (2.9). This approach is an easy one to implement if one knows when an element at yield remains plastic. In usual applications under a single monotonic load parameter all or most elements at yield do remain plastic and little if any internal unloading occurs. In our problem, however, internal unloading and reloading of elements is an essential feature of the analysis as the wheel rolls. Thus, there are always two possibilities of loading or unloading for the non-elastic elements. In the usual approach[7] all non-elastic elements are

either considered in the state of loading or an iterative technique is used. The first scheme is obviously not applicable to this problem and with the second approach there is always doubt about the rapidity or even the existence of the convergence of the process.

In the static approach to the problem by direct use of the static minimum principle and quadratic programming, the question of which plastic elements unload is handled automatically. This technique has been used previously on other problems[8–10].

The other feature of interest is the piecewise linear yield condition. Such conditions have, of course, been used in the past. Indeed, the Tresca yield condition can be regarded as a piecewise linear approximation to the Mises yield condition when the principal stress directions are known. However, in problems such as this where the principal directions are not known, the Tresca condition is also non-linear. In fact, there does not exist any closed isotropic piecewise linear yield surface when the principal directions are variable. Therefore, if we wish to use a piecewise linear yield surface we must pay the price of anisotropy in one form or another. Since the wheel does not have any fixed cartesian axes of reference, we have chosen to do this by making our piecewise linear approximation with reference to radial and tangential axes for each element.

A drawback to this approach is that a large number of linear equations are needed to define a yield surface, rather than a single non-linear one. However, this drawback is not severe as it appears. For a polygonal yield surface, at any given time, most of the domains are elastic. Therefore, even though we used 18 planes for the total description of the Tresca yield surface, at any one time a maximum of two of these were used for any element. Further, for the 12-element model there were never more than three elements plastic at any one time and the maximum total constraints for any time step was five.

The above disadvantage of the piecewise linear yield condition is trivial compared to its advantage for the present problem. If a non-linear yield condition is used with all other aspects remaining the same, the time integration step for finding the stress from the stress rate is equivalent to moving along the tangent, whereas the true solution for the model moves along the nonlinear yeild surface.

Figure 4 shows symbolically some of the things that might happen. The dashed curve represents the true solution which goes from A to B to C in two time steps. The obtained solution moves along the solid-line tangent AB' in the first time step.

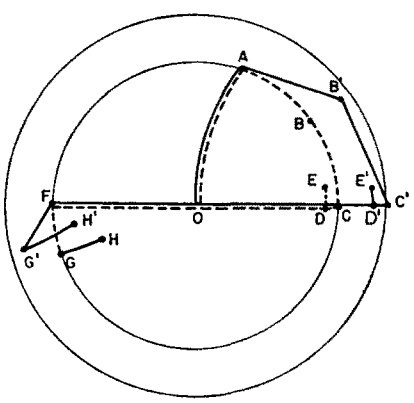

Fig. 4. Comparison between piecewise linear and non-linear yield conditions.

To evaluate the constraint at the second time step we must expand the yield curve so it goes through B. Thus the next time step is along the new tangent to C'.

From C to D both solutions unload and we have two choices to define our method. Suppose first that we shrink the yield surface with the stress point until it regains its original size. But then, if the true solution goes elastically from D to E, the obtained solution goes plastically from D' to E'. If this type of behavior happens in every revolution, we will predict no shakedown, whereas the true solution does shakedown.

Alternatively, if we do not shrink the yield surface, then in a path such as $DFGH$ the true solution would show plastic flow whereas the obtained one would not.

Since the essence of the problem is to predict shakedown, some change must be made in the above model and certainly a piecewise linear yield curve is one easy way of eliminating the difficulty.

REFERENCES

1. P. G. Hodge, Jr., A consistent finite element model for the two-dimensional continuum, *Ing. Archiv.* **39** 375–382 (1970).
2. W. Prager, The general theory of limit design, *Proc. 8th Int. Cong. Appl. Mech.*, Istanbul (1952) **2** 65–72 (1956).
3. A. McMahon and P. G. Hodge Jr., A simple finite element model for elastic–plastic plate bending, DOMIIT *Rep.* 1-46, Illinois Institute of Technology (1971) (Appendix A).
4. D. C. Drucker, A more fundamental approach to plastic stress–strain relations, *Proc. 1st U.S. Nat. Cong. Appl. Mech.*, Chicago (1951), 487–491. Edwards, Ann Arbor, Mich. (1952).
5. H. J. Greenberg, Complementary minimum principles for an elastic–plastic material, *Q. Appl. Math.* **7** 85–95 (1949).
6. P. Wolf, The simplex method for quadratic programming, *Econometrica* **27** (3), 382–389 (July 1959).
7. P. V. Marcal and I. P. King, Elastic–plastic analysis of two-dimensional stress systems by the finite element method, *Int. J. Mech.* **9** (3), 143–155 (1967).
8. C. T. Herakovich and P. G. Hodge, Jr., Elastic–plastic torsion of multiply-connected cylinders by quadratic programming, *Int. J. Mech. Sci.* **11**, 53–63 (1969).
9. P. G. Hodge, Jr., T. Belytschko and C. T. Herakovich, Quadratic programming and plasticity, *Computation Approaches Appl. Mech. ASME*, 73–84 (1969).
10. G. Maier, A quadratic programming approach for certain class of non-linear structural problems, *Meccanica* **3**, 121–130 (1968).

Абстракт — Определяется совместимая модель конечного элемента для круглого колеса на основе трехугольных и квазитрехугольных областей и кусочного поля линейного перемещения. Применяется принцип пластичности для минимума скорости напряжения, с целью решения задачи двухмерной сплошной среды с внутренней разгрузкой. Используется кусочное приближение условия течения Трески. Получаются упруго-пластические решения колеса, вращающегося по жесткой рельсовой пути, под влиянием своего собственного веса и веса втулки, для первых несколько оборотов перед достижением устойчивого условия. Показываются условия приспособления для колеса.